Front. Chem. Sci. Eng. 2019, 13(2): 350–359
https://doi.org/10.1007/s11705-018-1787-7

RESEARCH ARTICLE

Plasma-enabled healing of graphene nano-platelets layer

Xiuqi Fang[1], Carles Corbella (✉)[1], Denis B. Zolotukhin[1,2], Michael Keidar[1]

1 Department of Mechanical & Aerospace Engineering, George Washington University, Washington, DC 20052, USA
2 Department of Physics, Tomsk State University of Control Systems and Radioelectronics, Tomsk 634050, Russia

Abstract Graphene platelet networks (GPNs) were deposited onto silicon substrates by means of anodic arc discharge ignited between two graphite electrodes. Substrate temperature and pressure of helium atmosphere were optimized for the production of the carbon nanomaterials. The samples were modified or destroyed with different methods to mimic typical environments responsible of severe surface degradation. The emulated conditions were performed by four surface treatments, namely thermal oxidation, substrate overheating, exposition to glow discharge, and metal coating due to arc plasma. In the next step, the samples were regenerated on the same substrates with identical deposition technique. Damaging and re-growth of GPN samples were systematically characterized by scanning electron microscopy and Raman spectroscopy. The full regeneration of the structural and morphological properties of the samples has proven that this healing method by arc plasma is adequate for restoring the functionality of 2D nanostructures exposed to harsh environments.

Keywords graphene platelet networks, anodic arc discharge, plasma healing, scanning electron microscopy, Raman spectroscopy

1 Introduction

Plasma technology is a multidisciplinary field consolidated in industry for material synthesis and surface treatments [1−5]. One exciting facet of ionized gases is their versatility in biomedical applications: from cancer cells treatment through tissue regeneration, plasma medicine is a hot topic of research nowadays [6−9]. Nowadays plasma is actively used for various nanoparticle synthesis as well [10−13]. Nevertheless, the restoring faculty of plasmas is not limited to biological environments. Indeed, plasma healing is also an attractive feature in the case of inorganic materials and nanotechnology applications, especially when the prolonged operation of a system or device in a harsh environment is necessary [14]. An important example is constituted by the design of plasma Hall thrusters for small satellite propulsion, which currently involves the creation of smart materials containing nanotubes or graphene flakes. Such structures are intended to be fully operational with a minimal maintenance during long-term missions. Therefore, the optimal performance of microthrusters for satellites may include scheduled processes of component self-healing in flight, like recoating of thruster walls by adaptive plasmas and periodic synthesis of complex nanocomponents [15]. In the context of nanostructured materials, self-healing can be understood as a consequence of self-organization processes leading to a fully recovered functionality. For instance, structural self-repairing was observed on fractured boron nitride (BN) nanotubes, thereby proving that self-healing processes take place also in isolated nanomaterials [16].

Among all nanomaterial deposition techniques, synthesis by arc discharge is a valuable choice for the production of high-quality carbon nanoparticles and 2D nanostructures [17]. The main advantages consist of (1) the perfect cristallinity of the generated nanostructures due to the high temperatures reached in the arc column; (2) the high production yields from the ablated anode, and (3) the achievement of outstanding mechanical properties [18]. The possibility of depositing nanomaterials by arc plasma at low and high (atmospheric) pressures is an extra resource to control material properties. These samples can be produced in a systematic basis nowadays, and the development of self-healing recipes for devices including such nanomaterials would be very convenient. Regeneration of arc-grown carbon nanostructures, which has not been explored yet, will be a milestone for applications requiring self-restoring nanodevices by means of adaptive plasmas. Moreover, nanoparticle synthesis by arc plasmas is carried out in very short time intervals, thus justifying

Received August 12, 2018; accepted October 18, 2018

E-mail: ccorberoc@gwu.edu

that arc regeneration will constitute definitely a cost-effective technique for surface reparation.

Graphene platelet network (GPN) is a variety of carbon nanostructure which consists of randomly oriented few layers of graphene flakes. This work is focused on exploring the performance of GPNs in harsh environments, where their performance determines the lifetime of the system immersed in such environment. In this case, GPNs deposited on some substrates can face high enthalpy or high-energy fluxes. To this end, we have demonstrated GPNs re-growth or healing effect of the arc discharge GPNs synthesis. In this paper, we discuss the plasma-enabled healing of such graphene nano-platelets after their removal (or destruction) under different conditions. Four different procedures have been used to produce damage on the graphene layers deposited on silicon substrate, namely: (1) Thermal oxidation of graphene, which is commonly associated to high temperature processes in open atmosphere, like entrance of satellites from space into Earth atmosphere; (2) Overheating of substrate, condition met for instance in thermal treatments or high-speed tribology applications; (3) Exposition to a glow discharge, typical situation in plasma lithography or spaceships crossing ionosphere layers, and (4) Metallization by arc discharge, which can take place in components of thrusters. These treatments were intended to reproduce the conditions of a harsh atmosphere. After destruction of GPN samples, identical arc process has been used to re-grow graphene on the very same substrate. The structural and morphological properties of re-grown samples on a given substrate are characterized by scanning electron microscopy (SEM) and Raman spectroscopy.

2 Experimental

2.1 Synthesis of GPN by arc discharge

The GPN samples were synthesized in a cylindrical vessel by means of anodic arc discharge (Fig. 1). The deposition conditions are described in detail elsewhere [19,20]. Briefly, the anode consisted of a graphite rod of 3 mm in diameter, which faced a cathode of graphite with 10 mm of diameter. Inter-electrode gap was 4−5 mm. The ablated material comes from the anode and it constitutes the precursor for the nanoparticle growth. A Miller Goldstar SS300 power supply was used to ignite and support the arc, providing arc currents of up to 120 A with a voltage drop of approximately 30 V. Arc duration was equal or less than 5 s. The system was pumped down to a base pressure better than 0.1 Torr (1 Torr = 133.3 Pa) using a mechanical pump. All depositions were performed in helium atmosphere at 300−500 Torr and a substrate temperature of 800°C. Substrates, which consisted in monocrystalline silicon (c-Si) strips of ca. 7.5 mm × 75 mm, were heated ohmically and their temperatures were monitored using K type thermocouples attached to the backside of the wafer. GPNs were grown on substrates installed about 4 cm away from the electrodes' gap.

Intentional damaging of the graphene samples was produced by means of different techniques. The corresponding experimental setups are briefly described in section 3. In all cases, GPN were re-grown afterwards using the arc discharge. Surface morphology of the samples was observed by a Carl Zeiss Sigma VP Field Emission and FEI LV FEG SEM "Teneo". Raman spectroscopy by means of a Horiba LabRAM HR, operated at a wavelength of 532 nm, provided typical fingerprints of carbon nanostructures.

2.2 Characteristics of GPN samples

Figure 2 shows a representative SEM image and Raman spectrum of a GPN sample deposited on silicon at 800°C. The characteristic porous structure of GPN is observed in the SEM micrography. From the Raman spectrum we identify the three main peaks of such nanostructures, namely D (≈ 1350 cm^{-1}), G (≈ 1600 cm^{-1}) and G' (≈ 2700 cm^{-1}). Both D and G peaks appear relatively sharp and well-separated, as expected in carbon samples with significant concentration of sp^2-bonded carbon atoms [21].

G peak of a monolayer graphene is a single Lorentzian peak. In this situation, the full width at half maximum (FWHM) of G peak is around 24 cm^{-1}. The FWHM is

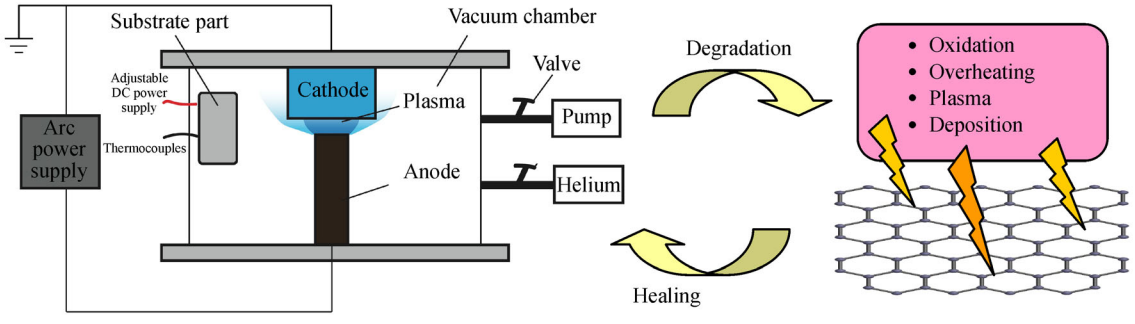

Fig. 1 Scheme of the reactor (not in scale) for synthesis of graphene nanoplatelets by anodic arc plasma discharge. Also, the transfer of GPN samples between the working stages of degradation environment and discharge healing is represented

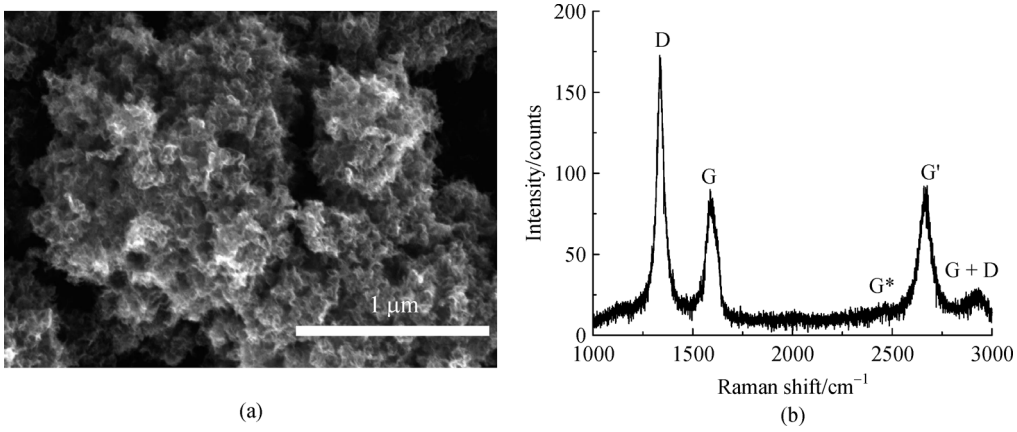

Fig. 2 (a) SEM top view of a GPN sample deposited by anodic arc discharge on c-Si at 800°C; (b) Raman spectrum of GPN showing the different carbon peaks. GPN structure is assessed by the features $\Delta G_{FWHM} \leqslant 100$ cm^{-1} and I(G')/I(G) ≈ 1

larger than 24 cm^{-1} as observed in Fig. 2, thus indicating presence of multilayered graphene. On the other hand, for monolayer graphene, the FWHM of G' peak is around 30 cm^{-1}. For multilayered graphene, G' peak is a convolution of multiple peaks yielding a larger overall FWHM for turbostratic multilayer graphene [22]. Such configuration consists of rotationally randomly stacked individual graphene layers. For triple- or four-layered graphene in Bernal stacking, the FWHM of G' peak is $\geqslant$ 100 cm^{-1} [22]. The graphene samples synthesized in this work at 800°C exhibit a G' band FWHM of about 100 cm^{-1}, implying that they consist of multilayered graphene layers.

The number of layers is also characterized by the I(G')/I(G) ratio. For pure monolayer graphene, the I(G')/I(G) ratio is bigger than 2, and normally it can achieve 3–5. The increase of the layer number in GPN causes the reduction of I(G')/I(G) ratio. The I(G')/I(G) ratio for double-layered graphene is about unity, whereas it decreases to 0.5−1 in the case of triple-layered graphene. Further increase in the number of layers results in a monotonic decrease in I(G')/I(G) ratio down to less than 0.1, which is a typical value for highly oriented pyrolitic graphite. The experiments conducted in the interval 700°C−800°C provided GPN showing a G' peak of less than 100 cm^{-1} in FWHM and I(G')/I(G) ≈ 1, which is consistent with 2−3 layer graphene sheets.

3 Results and discussion

3.1 Graphene oxidation in the atmosphere

Since graphene is a carbon allotrope, it can be removed from a substrate by burning graphene in the atmosphere. Thus, we connected the two ends of the GPN-coated silicon substrate to positive and negative terminals of a DC power supply (Fig. 3(a)). The system heated up quickly as a consequence of the large electric current circulating through the GPN layer. Thus, the GPNs structure on the surface reacted with oxygen according to the oxidation process $C + O_2 \rightarrow CO_2$, thus leaving an uncovered region between both terminals. The whole process has been schematized in Fig. 3(b). Representative SEM images and Raman spectra corresponding to the sample before the process, after the process (bare substrate), and after regeneration (healing) are shown in Fig. 3. Raman spectra of the samples before oxidation (pristine) and after re-growth show the D and G peaks of carbon, together with the G' peak characteristic of few-layer graphene nanostructures [23]. The sample without GPN deposit shows no carbon peaks, but an intense peak at about 500 cm^{-1} indicative of silicon substrate is detected instead.

3.2 Substrate overheating

Another way to remove the surface deposition of GPNs is to heat up the silicon substrate to about 900°C in vacuum. Afterwards, arc discharge plasma was used to generate again carbon flux for GPNs synthesis. With this vacuum annealing, the original GPNs deposition on the silicon surface cracked and peeled off. The silicon substrate has a melting temperature of 1414°C, and when the substrate is heated up to 900°C−1000°C, the surface of the substrate will gain some deformation due to thermal stress. A big challenge would consist in depositing again GPN on such a stressed substrate. Indeed, when such a stressed surface receives a beam with a large amount of carbon flux coming from the arc discharge plasma, the GPN might peel off due to adhesion issues. Three steps have been conducted using the same silicon substrate, namely step 1: GPNs grown on the silicon substrate; step 2: Overheat the substrate in vacuum and destroy the surface deposition; step 3: GPNs re-grown with arc discharge plasma. Both SEM and Raman spectra are shown in Fig. 4(a). An image of the silicon substrate after the overheat process in step 2 is shown in Fig. 4(b).

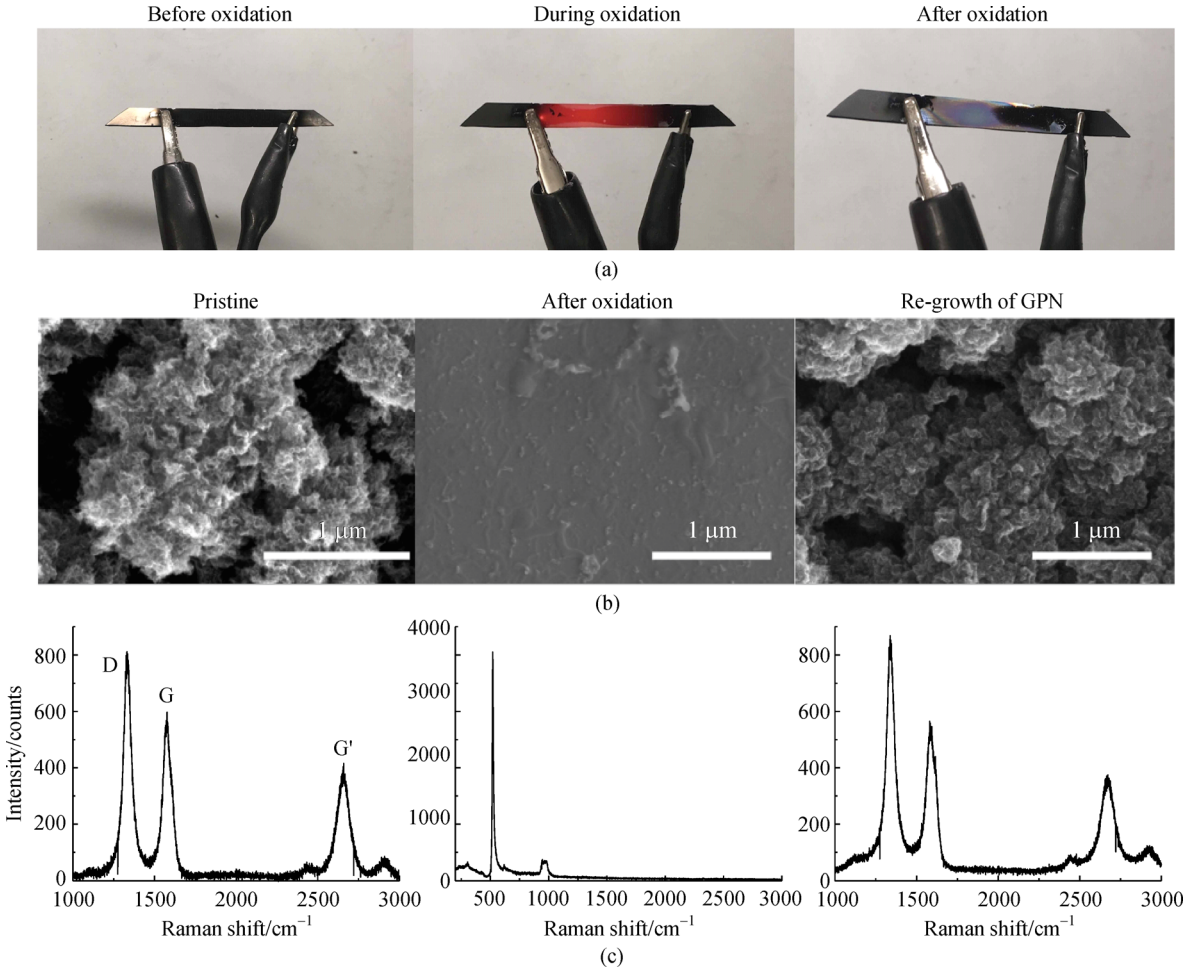

Fig. 3 (a) The oxidation process on the GPNs silicon substrate; (b) The healing process for the oxidation is shown by the corresponding SEM images and Raman spectra

3.2.1 Sequential thermal treatment

Furthermore, another experiment has also been done to prove that the healing effect by overheating could be repeated multiple times. Figure 5 shows a 5-step healing effect experiment performed with overheating the silicon substrate. In this Figure, step 2 and step 4 show the silicon substrate with destroyed GPNs surface and their corresponding Raman spectra. And step 3 and step 5 show the features of GPNs re-grown on the silicon surface together with the Raman spectra. This result is a strong evidence that GPN samples can be restored repeatedly as long as the substrate is in good conditions.

3.3 Glow discharge

Ionized gases at low pressure are widely used for film deposition, material etching and surface treatments such as functionalization [1,24]. In contrast with standard surface processes like chemical etching and flame treatments, glow discharge surface treatments show significant advantages: They constitute dry, clean and very flexible processes, inducing very low consumption of chemicals and other hazardous gases. Generally, plasma treatments only affect the surface material due to the limited penetration depth of the involved species. The experimental set up where AC glow discharge was used to damage GPN sample is shown in Fig. 6(a). This experiment was conducted in a stainless steel chamber (27 cm in length and 14.5 cm in radius) pumped with a mechanical pump to the residual air pressure of about 0.1 Torr. Argon gas was introduced in the chamber at a flow rate balancing the leak rate of the flange, so that the working gas pressure in the chamber remained at 0.1 Torr. The silicon substrate with GPNs was kept in the chamber during the glow discharge procedure for 10 mins. The treated substrate was analyzed by SEM and Raman spectroscopy. The pinkish purple colour shown in Fig. 6(b) is typical for argon glow discharge.

Figure 7 shows the SEM images and Raman spectra for this re-growth process. No substantial difference could be

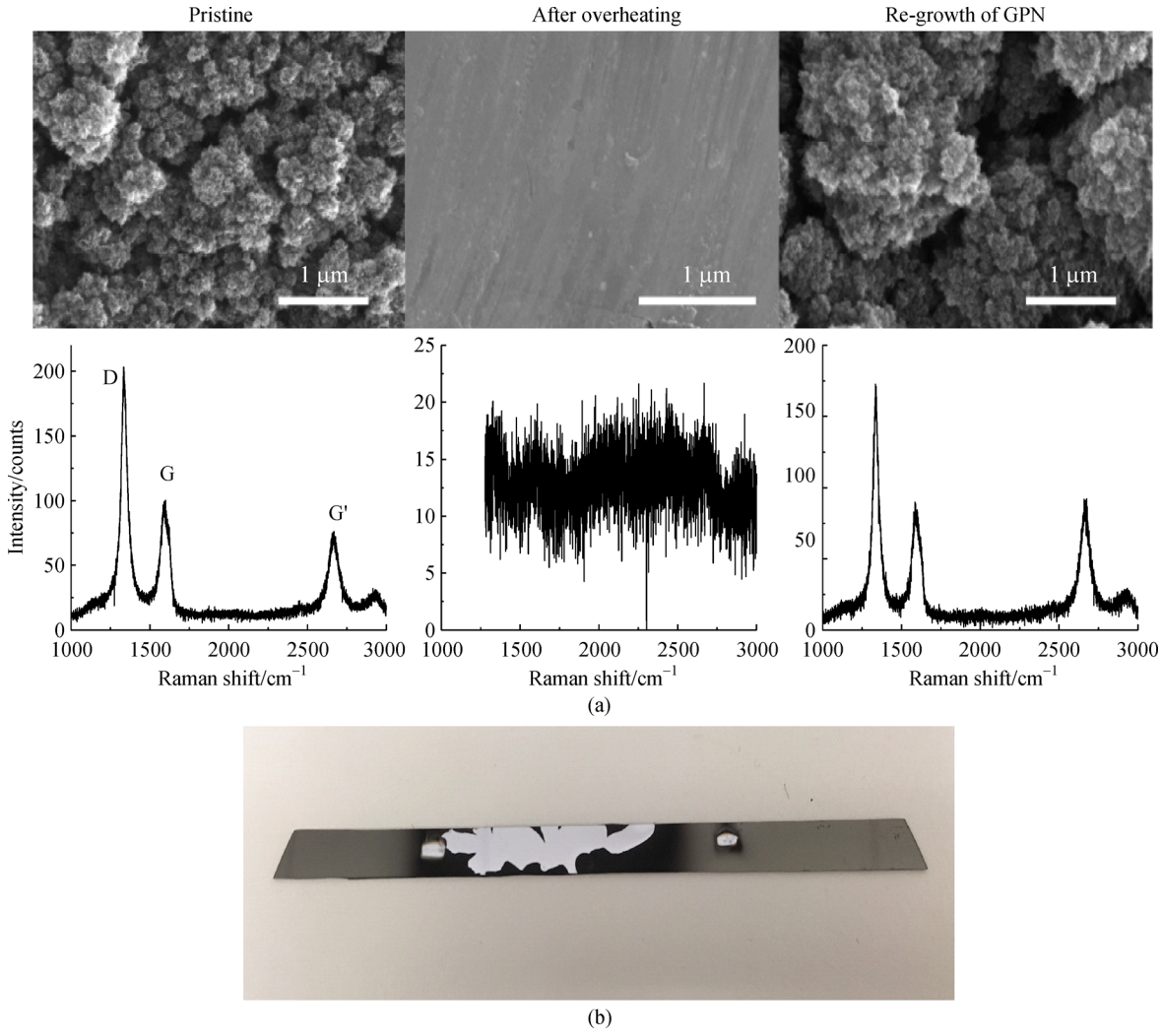

Fig. 4 (a) Graphene healing process with overheating the substrate step 1: GPNs grown on the silicon substrate; step 2: Overheat the substrate and destroy the surface deposition; step 3: GPNs re-growth with arc discharge plasma; (b) Sample just after the overheating process. The central region of exposed substrate was previously covered by a dark GPN coating

observed from these three SEM images, where the samples show the same GPNs porous surface morphology. But from the Raman spectrum, we can see that after the exposure to the glow discharge, the G' peak became less intense. The reduced intensity of G' after glow discharge could be attributed to defect formation in the GPN. This effect can be explained in terms of plasma-surface interaction. The argon glow discharge is composed of a combination of particles including ground-state, excited neutrals, ions and electrons. Bombardment of GPNs by ions accelerated in cathodic voltage drop of glow discharge will lead to degradation of GPNs surface. Also, the interaction of all these particles with the surface of the GPNs results in complex physical and chemical reactions, which change the surface properties of the GPNs. After using the same technique to re-grow the GPNs, Raman spectrum was observed to recover the initial status, i.e., all peak intensity ratios were restored.

3.4 Metallization

3.4.1 Microcathode arc thruster

Micro cathode arc thruster (μCAT) design for small space satellites is one of the major branches of study in our group [11,25]. With its short-term high voltage plasma plume, it can be used to provide thrust in space. In this experiment, it was used as a source to provide high-speed ions. Figure 8 shows a schematic of the basic system for μCAT. In this figure, we can see that a pair of electrodes, namely cathode and anode, is well aligned on the ceramic insulator substrate with inter-electrode gap covered by conductive carbon paint. The anode was made of Cu and the cathode was made of Ti, with the distance between the two electrodes being 2 mm.

During the experiment, the μCAT was controlled by a circuit, which periodically produces short voltage peaks of

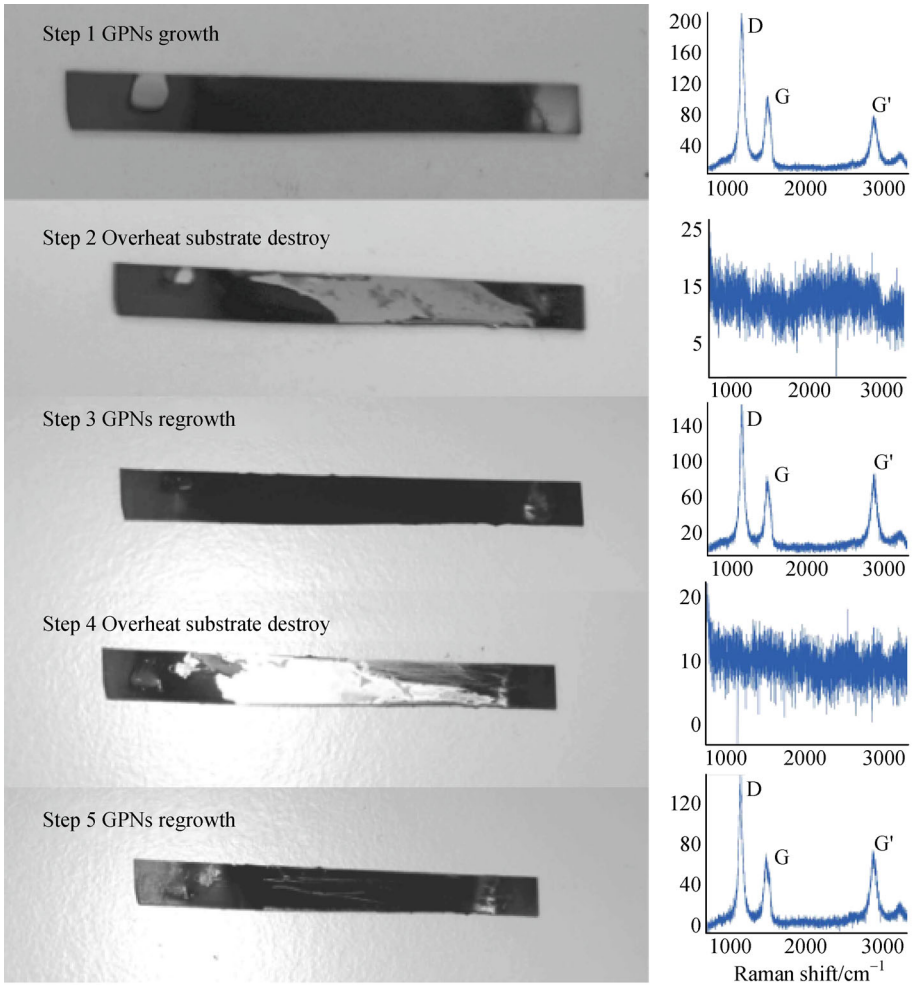

Fig. 5 5-step healing effect experiment done with overheating the silicon substrate. The Raman spectra on the right side show structural recovering after arc discharge deposition

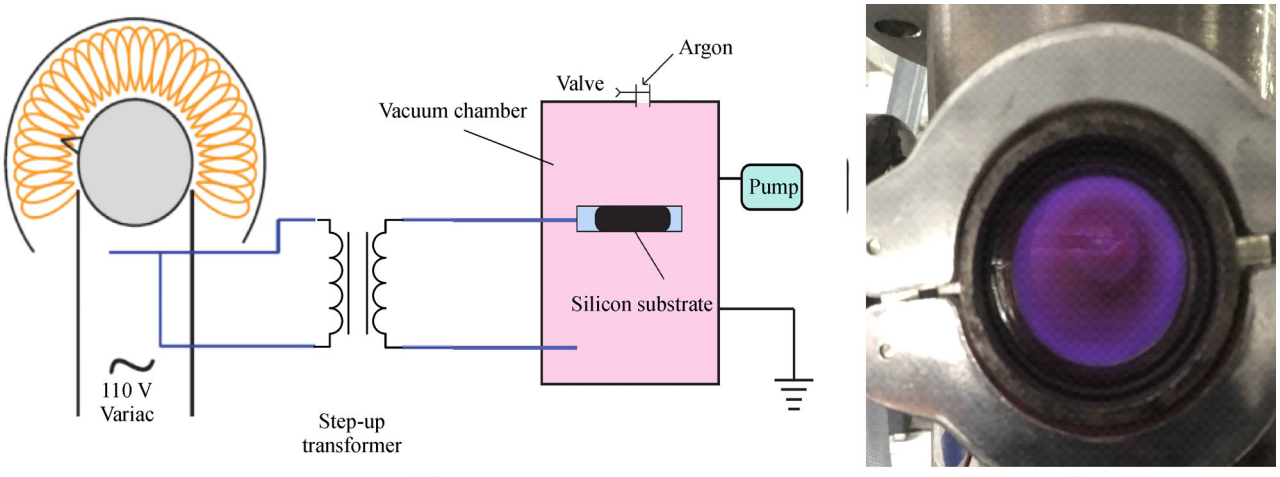

Fig. 6 (a) Experimental setup used to perform glow discharge surface treatment on silicon by means of AC argon plasma; (b) Image of the glow discharge emission taken from the reactor port view

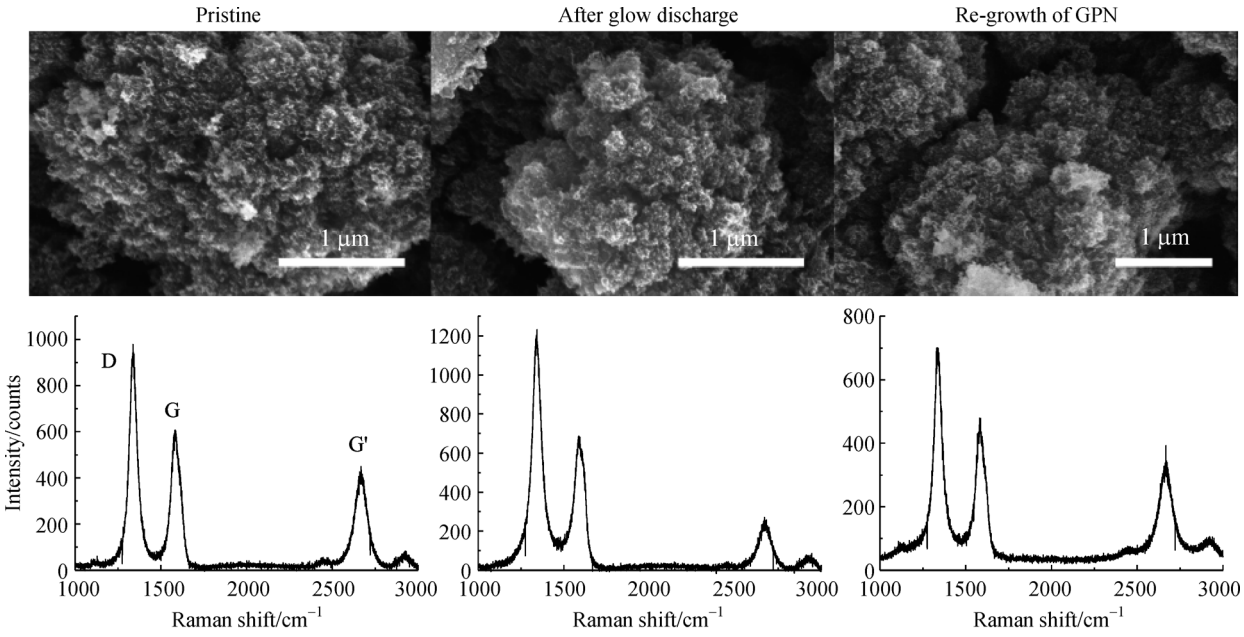

Fig. 7 SEM images and Raman spectra for graphene healing process with glow discharge

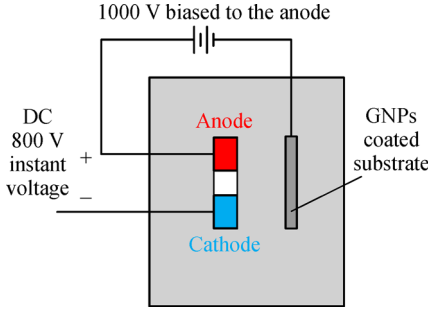

Fig. 8 Sketch of the experimental setup for the discharge ignition in the μCAT

about 800 V to ignite an arc between anode and cathode. The silicon substrate was negatively biased (–1000 V) with respect to the anode. Figure 9 shows the healing process for the μCAT coating. From both SEM image and Raman spectra, one can observe that the Ti coated the silicon substrate uniformly. Such Ti deposition on GPNs dominated over film erosion on GPNs caused by ion bombardment of the substrate. The dominant growth flux of Ti atoms came from cathode sputtering during the voltage pulses. Film thickness was estimated to be around 10 μm, which led to a decrease of I(G')/I(G) ratio by a factor two, as evidenced from Raman analysis. After metallization, same sample was exposed to the arc discharge plasma again. From the SEM image and Raman spectra, it is shown that the porous GPNs structure was deposited on the metal layer uniformly. This phenomenon proves that the re-growth process after surface metallization was successful.

3.4.2 Cathodic arc plasma coating

Cathodic arc plasma jet generated by vacuum arc has been used to provide a continuous flux of high-speed ions to bombard the surface of the silicon substrate. It is known that the ionized gas accelerates near the cathode spots hypersonically. The velocities of these ions produced by such arcs have a typical speed in the range of 1×10^4–3×10^4 m/s, which depend on the cathode material. The schematic of the vacuum chamber is shown in Fig. 10 (a). It consists of a stainless steel chamber with 45 cm in diameter and 64 cm in length. Mechanical and diffusion pumps were used to pump the chamber to a residual gas pressure of about 10^{-4} Torr. A titanium cylindrical cathode with a protrusion cone at the end has been used as Ti ion beam source. The vacuum chamber walls were used as an anode. The arc current was about 130 A and arc voltage was about 35 V. Cathode spots were stabilized on the

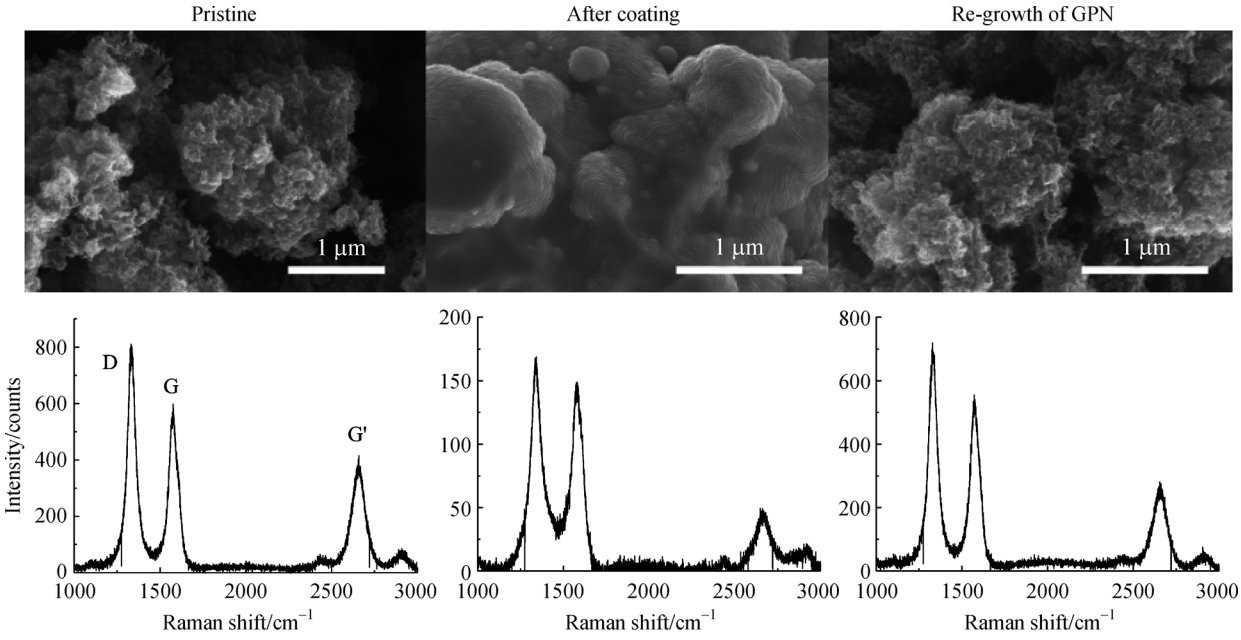

Fig. 9 The healing process for the μCAT coating shows that the initial network structure is recovered after re-growth of GPN onto the Ti-coated sample

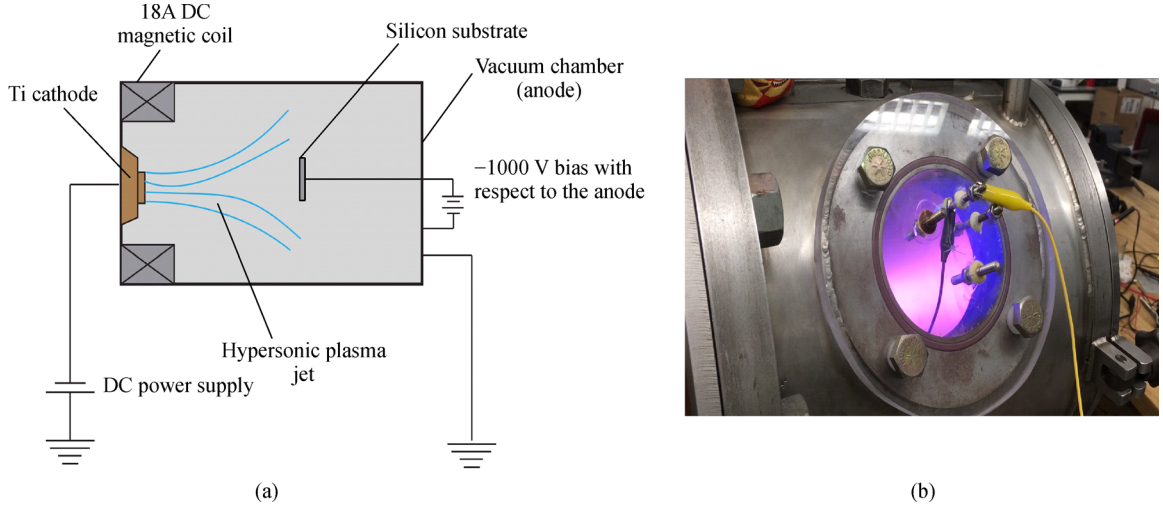

Fig. 10 (a) Schematic representation of the experimental setup; (b) Image of the cathodic arc plasma as taken from a port view of the chamber

protrusion by a permanent magnetic field created by a magnetic coil. The current through the magnetic coil was about 18 A.

The very short-time contact of the cathode with a mechanically triggered electrode ignited hypersonic plasma. During the experiment, the silicon substrate was negatively biased (–1000 V) towards the anode, so the ions could be accelerate towards the substrate leading to material sputtering in competition with deposition of titanium from the cathode. Here, ion sputtering of the substrate material was weaker and, instead, the dominant process during hypersonic plasma operation was Ti deposition. This resulted in a uniform Ti coating of the order of about 10 μm onto the substrate surface. In contrast with μCAT experiment, where similar coating was deposited, no Raman signal is observed here (Fig. 11). A possible reason of such difference may be the deposition of a thicker, denser and more homogeneous Ti layer than in the μCAT case. From both SEM image and Raman spectra, we can see the same re-growth phenomenon as in the previous experiment with μCAT. This further proves the healing capacity of arc plasma.

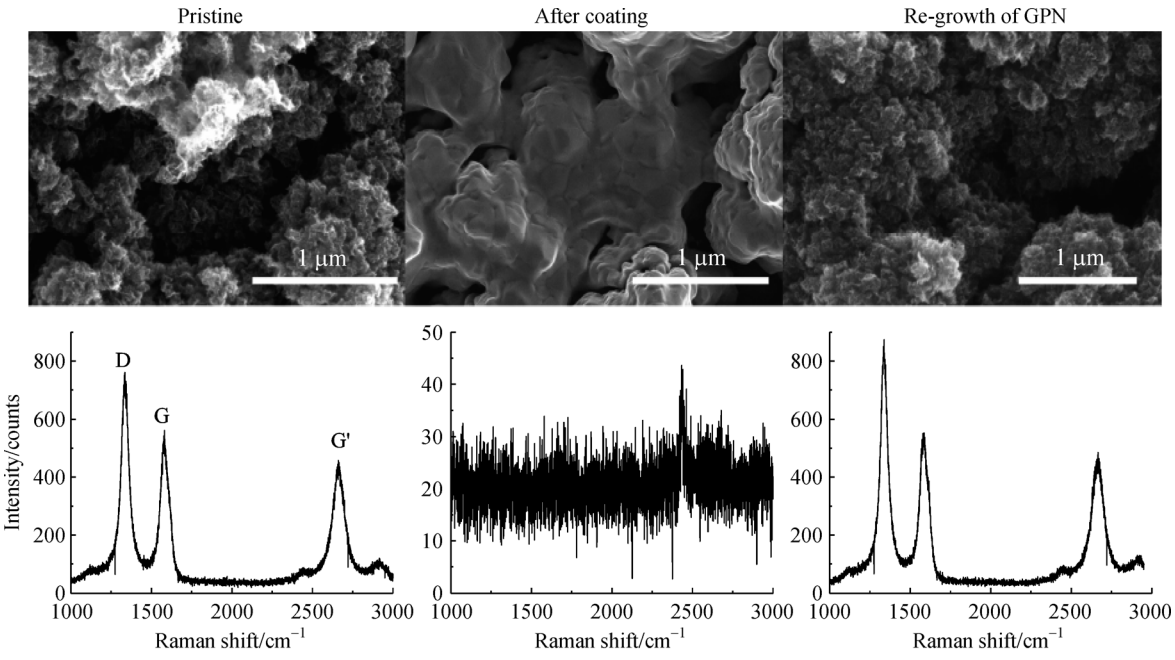

Fig. 11 SEM images and Raman spectra corresponding to the healing process for the cathodic arc plasma coating

4 Conclusions

In this study, graphene healing driven by arc discharge deposition has been tested in a number of scenarios. GPNs structures deposited on silicon substrates could be damaged or destroyed by different ways, namely oxidization, substrate overheating, glow discharge, and metal coating induced by arc plasma. Subsequently, the identical synthesis procedure could be used to re-grow GPNs on the same substrate in all the cases. Further experiment has also proved that this healing process could be repeated on the same substrate multiple times. However, these results validate the advantages of this method (anodic arc discharge) only for a specific material (GPN) and substrate (c-Si). Tests with further nanomaterials, such as MoS_2 or BN flakes on different substrates, are required to extend the performance of this healing method to new applications and alternative scenarios of material damaging or degradation.

Acknowledgements This work has been supported by Department of Energy under SBIR program through TechX Corporation and AFOSR.

References

1. Ohring M. Materials Science of Thin Films. 2nd ed. San Diego: Academic Press, 2002
2. Gordillo-Vázquez F J, Herrero V J, Tanarro I. From carbon nanostructures to new photoluminescence sources: An overview of new perspectives and emerging applications of low-pressure PECVD. Chemical Vapor Deposition, 2007, 13(6-7): 267–279
3. Keidar M, Beilis I I. Plasma Engineering: Applications from Aerospace to Bio- and Nanotechnology. London: Academic Press, 2013
4. Adamovich I, Baalrud S D, Bogaerts A, Bruggeman P J, Cappelli M, Colombo V, Czarnetzki U, Ebert U, Eden J G, Favia P, et al. The 2017 plasma roadmap: Low temperature plasma science and technology. Journal of Physics. D, Applied Physics, 2017, 50(32): 323001
5. Cvelbar U, Walsh J L, Černák M, de Vries H W, Reuter S, Belmonte T, Corbella C, Miron C, Hojnik N, Jurov A, et al. White paper on the future of plasma science and technology in plastics and textiles. Plasma Processes and Polymers, 2019, 16(1): e1700228
6. Fridman A, Friedman G. Plasma Medicine. Weinheim: Wiley, 2013
7. Graves D B. Low temperature plasma biomedicine: A tutorial review. Physics of Plasmas, 2014, 21(8): 080901
8. Keidar M, Yan D, Beilis I I, Trink B, Sherman J H. Plasmas for treating cancer: Opportunities for adaptive and self-adaptive approaches. Trends in Biotechnology, 2018, 36(6): 586–593
9. Bekeschus S, Favia P, Robert E, von Woedtke T. White paper on plasma for medicine and hygiene: Future in plasma health sciences. Plasma Processes and Polymers, 2019, 16(1): e1800033
10. Azarenkov N A, Denisenko I B, Ostrikov K N. A model of a large-area planar plasma producer based on surface wave propagation in a plasma-metal structure with a dielectric sheath. Journal of Physics. D, Applied Physics, 1995, 28(12): 2465–2469
11. Cheng Q, Xu S, Ostrikov K K. Single-step, rapid low-temperature synthesis of Si quantum dots embedded in an amorphous SiC matrix in high-density reactive plasmas. Acta Materialia, 2010, 58(2): 560–569
12. Volotskova O, Fagan J A, Huh J Y, Phelan F R Jr, Shashurin A, Keidar M. Tailored distribution of single-wall carbon nanotubes

from Arc plasma synthesis using magnetic fields. ACS Nano, 2010, 4(9): 5187–5192

13. Keidar M, Shashurin A, Volotskova O, Raitses Y, Beilis I I. Mechanism of carbon nanostructure synthesis in arc plasma. Physics of Plasmas, 2010, 17(5): 057101
14. Zavada S R, McHardy N R, Gordon K L, Scott T F. Rapid, puncture-initiated healing via oxygen-mediated polymerization. ACS Macro Letters, 2015, 4(8): 819–824
15. Levchenko I, Xu S, Teel G, Mariotti D, Walker M L R, Keidar M. Recent progress and perspectives of space electric propulsion systems based on smart nanomaterials. Nature Communications, 2018, 9(1): 879
16. Golberg D, Bai X D, Mitome M, Tang C C, Zhi C Y, Bando Y. Structural peculiarities of *in situ* deformation of a multiwalled BN nanotube inside a high-resolution analytical transmission electron microscope. Acta Materialia, 2007, 55(4): 1293–1298
17. Iijima S. Helical microtubules of graphitic carbon. Nature, 1991, 354(6348): 56–58
18. Shashurin A, Keidar M. Synthesis of 2D materials in arc plasmas. Journal of Physics. D, Applied Physics, 2015, 48(31): 314007
19. Fang X, Shashurin A, Teel G, Keidar M. Determining synthesis region of the single wall carbon nanotubes in arc plasma volume. Carbon, 2016, 107: 273–280
20. Fang X, Donahue J, Shashurin A, Keidar M. Plasma-based graphene functionalization in glow discharge. Graphene, 2015, 4(1): 1–6
21. Ferrari A C, Robertson J. Interpretation of Raman spectra of disordered and amorphous carbon. Physical Review. B, 2000, 61 (20): 14095–14107
22. Ferrari A C, Meyer J C, Scardaci V, Casiraghi C, Lazzeri M, Mauri F, Piscanec S, Jiang D, Novoselov K S, Roth S, et al. Raman Spectrum of graphene and graphene layers. Physical Review Letters, 2006, 97(18): 187401
23. Ferrari A C, Basko D M. Raman spectroscopy as a versatile tool for studying the properties of graphene. Nature Nanotechnology, 2013, 8(4): 235–246
24. Lieberman M A, Lichtenberg J A. Principles of Plasma Discharges and Material Processing. 2nd ed. Hoboken: Wiley, 2005
25. Zolotukhin D B, Keidar M. Optimization of discharge triggering in micro-cathode vacuum arc thruster for CubeSats. Plasma Sources Science & Technology, 2018, 27(7): 074001